

Experimental Results from R245fa Ejector Chiller

J. Mahmoudian¹, A. Milazzo^{1*}, I. Murmanskii² and A. Rocchetti¹

¹DIEF- Department of Industrial Engineering, University of Florence – via S.Marta, 3, 50139 Florence (ITALY)

²Ural Power Engineering Institute, Ural Federal University, Ekaterinburg, Russia

*Corresponding author: adriano.milazzo@unifi.it

Abstract

This paper presents new experimental results from the DIEF prototype ejector chiller, which is operating since 2011 and has undergone several refinements, as discussed elsewhere. The prototype features a modified CRMC design of the ejector and a cooling power of a 40 kWf. The working fluid, R245fa, has favourable thermodynamic properties (e.g. dry expansion and moderate pressure at generator) and allows sub-zero temperatures at evaporator. Therefore, even if the prototype was designed for 5°C evaporation temperature, a set of low temperature tests has been carried on. The results show that the CRMC ejector chiller is rather flexible with respect to off-design conditions and, once specifically optimized, could be a candidate for sub-zero applications, unfeasible for water-lithium bromide absorption chillers.

Keywords: Ejector chiller, CRMC, R245fa, Experimental.

Introduction

Ejector chillers are often claimed [1,2] as promising competitors for absorption chillers in the heat-powered refrigeration market, but their energy efficiency normally turns out to be lower. Nonetheless, they could be competitive in those applications where the input energy is basically costless (waste heat, solar). In these cases, ejector chillers may offer a low investment cost and a robust operation. From this point of view, steam would be the obvious choice as a working fluid, being costless, safe for operators and environment and available everywhere. In any industrial environment where steam is produced for other purposes, steam ejectors are unrivalled as simple and relatively effective means for refrigeration [3].

However, synthetic fluids may have some peculiar advantages. A first point is undoubtedly the volumetric cooling capacity. Water, notwithstanding its outstandingly high latent heat, has a very low vapour density at low temperature (Table 1), while common refrigerants have much higher values. The influence of volumetric cooling capacity on the size of an ejector chiller is not as straightforward as in vapour compression cycles featuring volumetric compressors. However, the values in Table 1 suggest that a steam ejector chiller is likely to be much more bulky for a given cooling capacity.

Table 1 – Fluid properties – comparison

Fluid	Latent heat [kJ/kg]	Vapour density [kg/m ³]	Volumetric cooling capacity [kJ/m ³]	Saturation pressure [bar]	
				@ 0°C	@ 100°C
Water	2501	0.00485	12.13	0.00612	1.014
R134a	198.6	14.43	2866	2.929	39.72
R245fa	204.5	3.231	660.7	0.5295	12.65
R1233zd(E)	204.9	2.820	577.7	0.4788	10.50

Fluid properties calculated via NIST REFPROP [4]

A second point is the operating pressures within the various parts of the chiller. Water has low saturation pressure at all temperature levels encountered along an ejector cycle. The

generator, if operated e.g. at 100°C, is at ambient pressure, but the evaporator typically works below 1 kPa. This requires very accurate sealing of the circuit. On the other hand, R134a has a rather high pressure at typical generator temperatures (Table 1), which makes the operation and the energy consumption of the generator feed-pump more troublesome. R245fa is a good compromise, as it goes slightly below ambient pressure at evaporator but remains within a moderate 12.6 bar at 100°C.

A third point is the slope of the upper limit curve on the temperature – entropy diagram. R245fa and R1233zd have an inward slope of the limit curve. This means that the primary nozzle and the whole ejector are free from liquid condensation even if the expansion starts on the limit curve with no superheating. R134a and water, on the other hand, have a “wet expansion” and therefore they need a substantial superheating at generator exit.

A last point that favours synthetic fluids is the absence of icing, which may represent a serious problem for steam ejector chillers and limits their operation to above zero.

On the other hand, F-gas regulations limit the use of fluids with GWP>150 in Europe and other countries have similar limitations. Therefore R245fa (GWP = 950) could prove unusable in most applications. HFOs (Hydro-Fluoro-Olefins) are currently proposed as “drop-in” replacement of HFCs [5]. Among them, R1233zd has similar thermodynamic properties (see Table 1) and hence experimental results gathered with R245fa may be an indication for the performance of an equivalent system using the low-GWP alternative fluid. Everything considered, we decided to continue our experimental activity on the existing prototype and to substitute R245fa with R1233zd in the near future.

R245fa was tested as a working fluid for an ejector chiller in 2006 by Eames et al. [6]. The ejector was a CRMC design, i.e. the flow sections were calculated by imposing a constant rate of deceleration along the mixer/diffuser. The experimental results showed that, for saturation temperatures of 110°C at generator and 10°C at evaporator, the COP could be as high as 0.47, with a critical condenser temperature of 32.5°C. Raising generator temperature to 120°C decreased the COP to 0.31, but the critical condenser temperature increased to 37.5°C. Superior performance of CRMC design has been recently confirmed in [7]. Here we present further experimental results from a modified version of the CRMC ejector, which has been tested on a wide range of operating conditions.

Experimental set up

Our ejector was designed starting from a scaled-up version of Eames’ design, introducing a bell-shaped end on the suction side and a conical outlet on the discharge side. The ejector has 3 flanged sections manufactured in aluminium, in order to allow for a good surface finish. A Ka roughness of the internal surface from 4 to 6 microns was measured in different locations. The primary nozzle can be moved axially in order to optimize the entrainment.

The present arrangement is the result of a long refinement work, as described in previous publications [8,9]. Main geometrical data of the ejector in the present configuration are reported in Table 2.

Table 2 – Main geometrical parameters of the ejector

	Nozzle	Diffuser
Throat diameter [mm]	10.2	31.8
Exit diameter [mm]	20.2	108.3
Length [mm]	66.4	950
Material	Aluminum	Aluminum

Nine ports have been drilled perpendicularly to the ejector inner surface in order to measure the local static pressure. The holes are placed at 100 mm intervals, starting at 50 mm from the inlet flange of the ejector, as shown in Fig. 1. The primary nozzle can be moved forward and backward from a reference position having the nozzle exit plane coincident with the inlet plane of the bell-shaped inlet of the suction chamber.

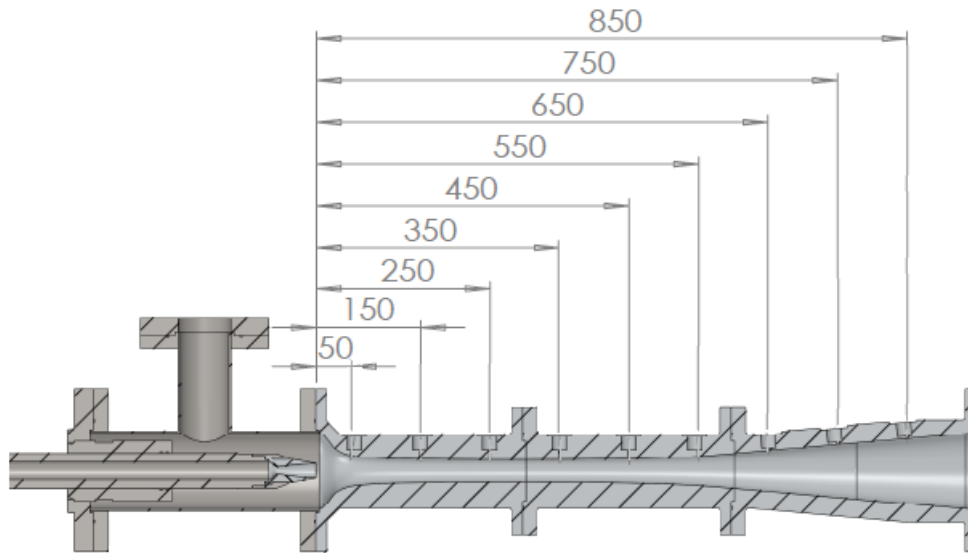


Fig. 1 – CRMC ejector with static pressure ports and movable primary nozzle.

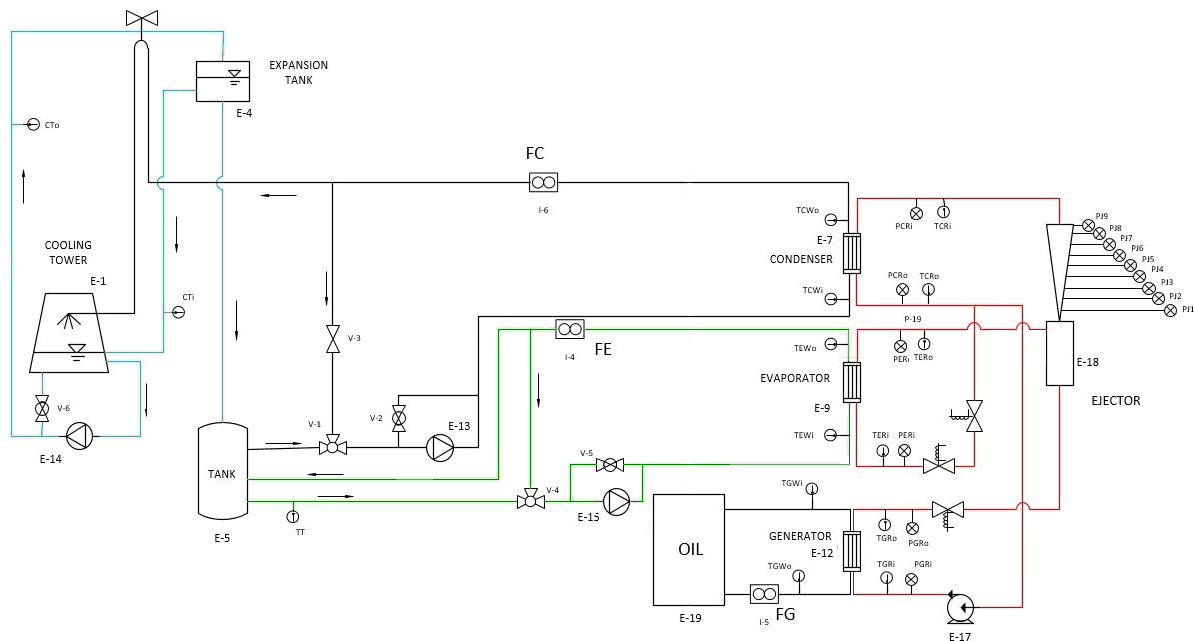


Fig. 2 – Experimental set-up

The ejector is part of a heat-powered refrigeration system (Fig. 2) designed to give 40 kW of refrigeration to a chilled water stream entering at 12 and exiting at 7°C. In the original set-up the heat source was hot water at 90 – 100°C. Now a thermal oil electric heater is used as heat source, in order to explore a wider temperature range. An evaporative cooling tower discharges the system power into the ambient air outside the laboratory. The cooling tower receives the warm water directly from the condenser and feeds a buffer tank, in order to have a stable water source at near ambient temperature. The tank water is used to give the heat

load to the evaporator and to cool the condenser. By-pass branches are used to regulate the temperature at evaporator and condenser inlets. Mass flow meters and temperature sensors are mounted on the condenser and evaporator water circuits, in order to have the instantaneous energy balance of the system. Temperature and pressure sensors are mounted in all the significant points along the refrigerant circuit, while 9 pressure probes are mounted along the ejector as above mentioned. The specifications of the main sensors are reported in Table 3.

Table 3 – Specifications of the sensors and data acquisition

Instrument	Model/type	Position	ADC Module	Total uncertainty
Piezoreistive pressure transducer	PA25HTT 0-30 bar	Diffuser	NI9208	$\pm(0.1\% + 0.22\%$ FS)
	PR23R 0.5-5 bar	Evaporator	NI9208	$\pm(0.1\% + 0.22\%$ FS)
	PA21Y 0-30 bar	Generator, Condenser	NI9208	$\pm(0.08\% + 1.0\%$ FS)
Resistance temperature detector	Pt100	Whole Plant	NI9216, NI9217	$\pm 0.25^{\circ}\text{C}$
Thermocouple	T	Cooling Tower, Tank	NI9213	$\pm 1.0^{\circ}\text{C}$
Electromagnetic water flowmeters	Endress Hauser Promog 50P	Condenser	NI9219	$\pm(0.5\% + 0.04\%$ FS)
Compact Rotamass mass flowmeter	YOKOGAWA RCCT28	Evaporator	NI9219	$\pm(0.05\% + 0.1\%$ FS)
Vortex flowmeter	YOKOGAWA YF105	Generator	NI9219	$\pm(0.8\% + 0.1\%$ FS)

All the experimental points have been measured after at least 15 minutes of stable operation and are averaged over 5 minutes. The generator feed pump has a variable frequency control, but has been always operated at 100% rotation speed.

Results and discussion

All saturation temperatures reported below are calculated from the pressure measured on top of each plate heat exchanger via NIST REFPROP functions. The experiments presented herein are all referred to a saturation temperature of 95°C at generator, corresponding to the maximum power of the thermal oil electric heater.

The expansion valve is manually operated in order to fix the saturation temperature at the evaporator.

For each evaporator condition, the water temperature at condenser inlet is raised by 0.3°C intervals until the cooling power vanishes. The results are reported in terms of COP v/s saturation temperature at condenser.

The higher generator temperature used in these new tests produces lower COP values with respect to those reported in [3]. Furthermore, entrainment ratio and COP have been negatively influenced by the decision to keep chilled water temperature constant (12°C at inlet and 7°C at outlet) throughout the test campaign. This causes a high superheating at evaporator exit, specially at low evaporation temperature, and hence a low vapour density at secondary inlet. On the other hand, the relatively high water temperature avoids any risk of icing.

a) Effect of evaporator saturation temperature

The system behaviour at reference working condition is shown in Fig. 32. The COP (Fig. 3a) shows a fairly constant value until point 5 and a sudden decrease at point 6, corresponding to a saturation temperature at condenser T_{C-sat} slightly above 31°C . Correspondingly, the static pressure at the wall measured by the 9 pressure transducers shows two easily distinguishable shapes (Fig. 3b). Note that the lines connecting the points are drawn only as a visual aid and do not represent the real pressure variation along the ejector. The curves from 1 to 5 all show a common pressure value at transducers 1,2 and 3, i.e. until 250 mm from the ejector inlet. The transition between supersonic and subsonic flow is apparently located between 250 and 350 mm, all sensors downstream being sensitive to the condenser pressure. Note that the diffuser throat is located around 300 mm.

The two further points 6 and 7 show a completely different behaviour, featuring a sharp pressure increase before 250 mm and then a slower increase before 550 mm. Note that in any case the pressure recovery after 550 mm is null or even negative, which raises some concern about the design of the final part of the ejector.

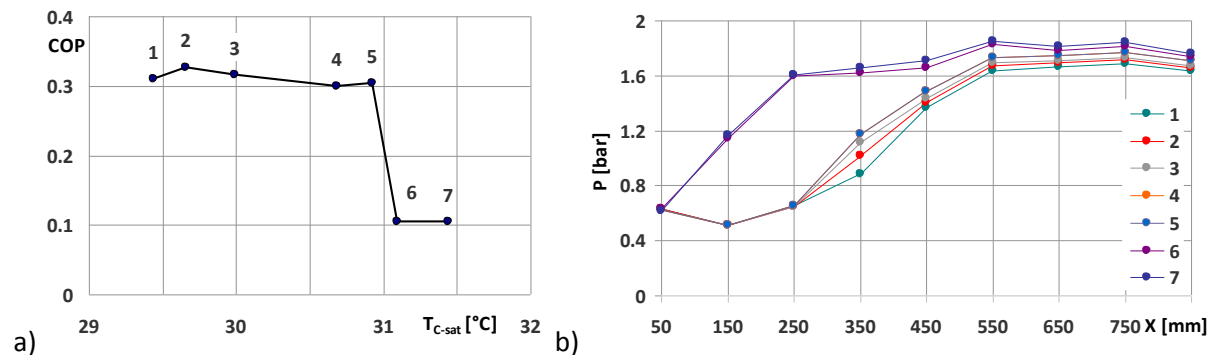


Fig. 3 – COP and static pressure at wall along the ejector @ $T_{E-sat} = 5^{\circ}\text{C}$ and $NXP = 0$ mm

Points 6 and 7 show that, once the critical pressure has been surpassed, a small secondary flow can still survive to a further small condenser pressure increase. This part of the curve is usually truncated and is obviously not significant as a practical working condition. However, it is a quite general feature and represent a safety margin before a dangerous backflow.

When the evaporation temperature is lowered to 0°C , the behaviour changes as shown in Fig. 4. Note the lower values of COP and critical pressure. Again, the operation continues beyond the critical condenser temperature even if at very low efficiency.

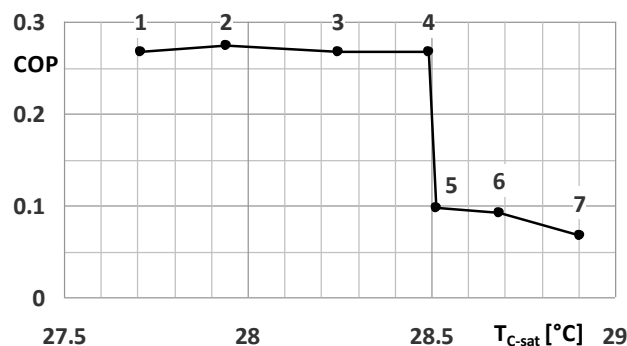


Fig. 4 – COP @ $T_{E-sat} = 0^{\circ}\text{C}$ and $NXP = 0$ mm

Further reduction of the evaporation temperature to -5°C obviously gives an even lower COP and a very low range in terms of condenser temperature (Fig. 5a). However, the ejector proves to

be able to reach such a low value of suction pressure (Fig. 5b), even if designed for a quite different working condition. The transition between on-design and off-design operation is abrupt as in Fig. 3b.

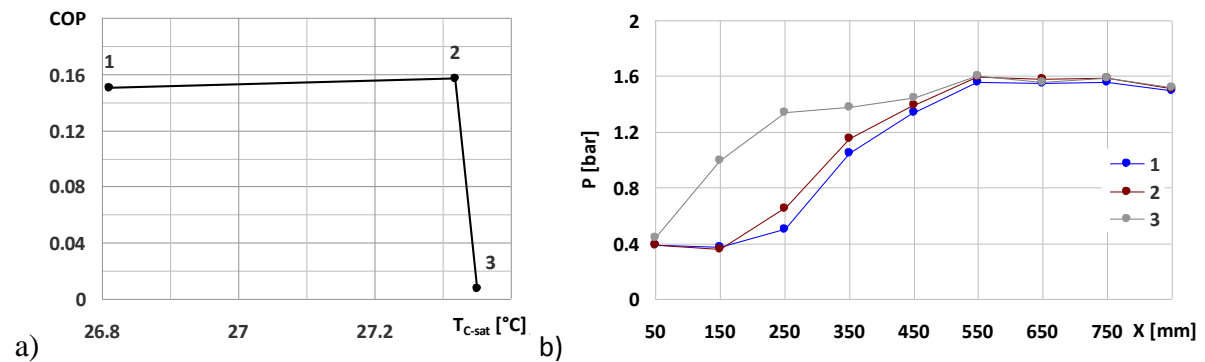


Fig. 5 – COP and static pressure at wall along the ejector @ $T_{E-sat} = -5^{\circ}\text{C}$ and $NXP = 0$ mm

a) Effect of nozzle position

According to the widely accepted model presented by Huang et al. [10] for the supersonic ejector operation, the entrainment ratio should be influenced by the area available for the secondary flow in the section where this latter reaches its sonic velocity. According to this view, an increase in the distance between the nozzle exit and the minimum area of the diffuser should cause an increase in the exit cone of the primary flow and hence a decrease in the secondary flow rate. A more realistic view sees the ejector as a momentum exchanger between the supersonic primary flow and the slow secondary flow [11]. Accordingly, an increased mixing length between the motive and entrained flow should actually increase the entrainment.

In the case of present measurements, the situation is complicated by the absence of a cylindrical mixing zone within the diffuser. The available flow section changes continuously from the inlet to the throat of the CRMC diffuser. This makes the effect of the nozzle exit position quite unpredictable.

The experimental results (Fig. 6) show that the COP measured at on-design conditions is actually reduced by a very modest amount, if any. The critical condenser temperature, on the other hand, is significantly decreased. This may be explained considering that a withdrawal of the nozzle causes a corresponding retraction along the diffuser of the section where the flow is fully supersonic. Hence, the working condition that causes this section to overcome the diffuser throat is anticipated.

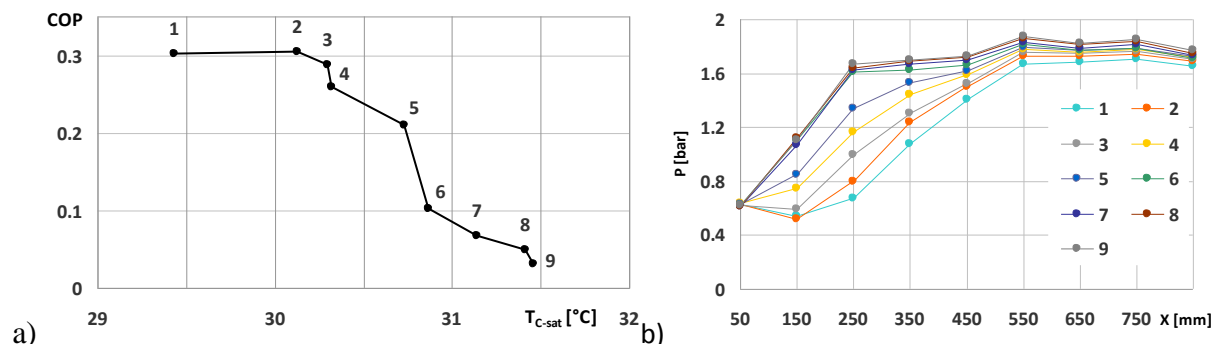


Fig. 6 – COP and static pressure at wall along the ejector @ $T_{E-sat} = 5^{\circ}\text{C}$ and $NXP = 5$ mm

Another interesting point is the completely different shape of the decreasing part of the COP line. In this case, the transition seems to take place in a rather gradual way, in lieu of a sharp decrease as shown in Figs. 3-5. Correspondingly, the pressure lines in Fig. 6b are equally

spaced between the lowest one, surely representing an on-design condition, to the highest. It could be concluded that in this configuration the ejector, given a longer space for momentum exchange between the flows, is more affected by the increased discharge pressure, but at the same time may accommodate this disturbance with a higher flexibility. As explained in [11], the primary flow undergoes a sequence of oblique shocks starting from the interface between super and subsonic flow and featuring multiple reflections on the axis and on the interface. The sequence of sharp descents and less inclined parts visible in Fig. 6b could be a trace of the interaction between the oblique shocks and the ejector profile. Obviously a more detailed analysis would be necessary before drawing a conclusive description of this phenomenon.

Conclusions

The CRMC ejector chiller working with R245fa has proved to be effective even at relatively low evaporation temperatures. If specifically designed, an ejector featuring the same criteria and structure could be suitable for new applications. The experimental activity will continue on the same prototype using a low GWP replacement fluid, i.e. R1233zd, that requires minor modifications to the chiller. Hopefully this activity will contribute to establish the feasibility of a robust and low-cost heat powered refrigeration system, featuring an environmentally safe refrigerant and operating below 0°C with a moderate temperature heat input.

Acknowledgements

The research leading to these results has received funding from the MIUR of Italy within the framework of PRIN2015 project «Clean Heating and Cooling Technologies for an Energy Efficient Smart Grid». A special thank goes to Mr. Furio Barbetti, who has given a precious contribution to the design and realization of the experimental set-up.

References:

- [1] Besagni, G., Mereu, R., Inzoli, F., “Ejector refrigeration: A comprehensive review”, *Renewable and Sustainable Energy Reviews*, 2016, doi.org/10.1016/j.rser.2015.08.059
- [2] Chen, X., Omer, S., Worall, M., Riffat, S., “Recent developments in ejector refrigeration technologies”, *Renewable and Sustainable Energy Reviews*, 2013, doi.org/10.1016/j.rser.2012.11.028
- [3] Power, R.B., *Steam Jet Ejectors for the Process Industries*, Author-Publisher, 1994, www.jetwords.com
- [4] NIST REFPROP, Reference Fluid Thermodynamic and Transport Properties Database, version 9.1, 2018. <https://www.nist.gov/srd/refprop>.
- [5] Fang, Y., Croquer, S., Poncet, S., Aidoun, Z., Bartosiewicz, Y., “Drop-in replacement in a R134 ejector refrigeration cycle by HFO refrigerants”, *International Journal of Refrigeration*, 2017, doi.org/10.1016/j.ijrefrig.2017.02.028
- [6] Eames, I.W., Ablwaifa, A.E., Petrenko V., “Results of an experimental study of an advanced jet-pump refrigerator operating with R245fa”, *Applied Thermal Engineering*, 2007, doi.org/10.1016/j.applthermaleng.2006.12.009
- [7] Kittratana, B., Aphornratana, S., Thongtip, T., Ruangtrakoon N., “Comparison of traditional and CRMC ejector performance used in a steam ejector refrigeration”, *Energy Procedia*, 2017, doi.org/10.1016/j.egypro.2017.10.229
- [8] Milazzo, A., Rocchetti, A., Eames, I.W., “Theoretical and experimental activity on ejector refrigeration”, *Energy Procedia*, 2014, doi.org/10.1016/j.egypro.2014.01.130
- [9] Mazzelli F., Milazzo A., “Performance analysis of supersonic ejector cycle working with R245fa”, *International Journal of Refrigeration*, 2015, doi.org/10.1016/j.ijrefrig.2014.09.020

- [10] Huang, B., Chang, J., Wang, C., Petrenko, V. “A 1-D analysis of ejector performance”, *International Journal of Refrigeration*, 1999. [doi.org/10.1016/S0140-7007\(99\)00004-3](https://doi.org/10.1016/S0140-7007(99)00004-3)
- [11] Grazzini, G., Mazzelli, F., Milazzo, A., “Physics of the Ejectors” in *Ejectors for Efficient Refrigeration - Design, Applications and Computational Fluid Dynamics*, Springer, 2018. doi.org/10.1007/978-3-319-75244-0